

**INTERDISCIPLINARY APPROACH TO DEFORMATION
ANALYSIS IN ENGINEERING, MINING, AND GEOSCIENCES
PROJECTS BY COMBINING MONITORING SURVEYS
WITH DETERMINISTIC MODELING
PART II**

Anna Szostak-Chrzanowski

Department of Geodesy and Geomatics Engineering
Canadian Centre for Geodetic Engineering
University of New Brunswick P.O.

K e y w o r d s: deformation analysis, integrated monitoring, engineering, mining, finite element method.

A b s t r a c t

This presentation, after a general review of problems and literature related to the analysis of deformations, summarizes the author's achievements and applications of the integrated deformation analysis in engineering, mining and geosciences projects.

**INTERDYSYPLINARNE PODĘJCIE DO ZINTEGROWANEJ ANALIZY DEFORMACJI
DOTYCZĄCEJ PROBLEMÓW INŻYNIERYJNYCH, GÓRNICZYCH
I GEOFIZYCZNYCH PRZEZ POŁĄCZENIE POMIARÓW GEODEZYJNYCH
Z ANALIZĄ DETERMINISTYCZNĄ
CZEŚĆ II**

Anna Szostak-Chrzanowski

Centrum Geodezji Inżynierijnej
Uniwersytet New Brunswick
Fredericton, Canada

S l o w a k l u c z o w e: analiza deformacji, zintegrowany monitoring, inżynieria, górnictwo, metoda elementów skończonych.

S t r e s z c z e n i e

Niniejsze opracowanie zawiera – po przedstawieniu przeglądu problemów i literatury z zakresu analizy deformacji – podsumowanie osiągnięć autorki wraz z omówieniem zastosowań przemysłowych zintegrowanej analizy deformacji obiektów inżynierijnych, górniczych i geofizycznych.

1. Introduction

This presentation presents some of the author's applications using the interdisciplinary approach to integrated deformation analysis in engineering, mining and geosciences projects by combining monitoring surveys and deterministic analysis (numerical modeling using finite element method). The combination of monitoring and numerical modeling of deformations is essential for studying the processes occurring in engineering structures and in rock mass at the construction and post-construction stages.

Safety, economy, efficient functioning of man-made structures and fitting of structural elements, environmental protection, and development of mitigation measures in case of natural disasters require good understanding of causative factors and the mechanism of deformations, which can be achieved only through proper monitoring and analysis of deformable bodies. Development of new methods and techniques for monitoring and analysis of deformations and development of methods for optimal modeling and prediction of deformation is the subject of intensive international studies of several professional and scientific groups.

The author has developed interdisciplinary approach to modeling, physical interpretation, and prediction of deformations. The approach is based on a combination (integration) of deterministic modeling (prediction) of deformations with the monitoring results obtained from geodetic and/or geotechnical measurements of displacements and deformations of the investigated object. Research has focused on the development of an analytical approach to the identification of physical parameters of the deformable material, to gain information on the material model, and to enhance understanding of the deformation mechanism of the investigated object (rock mass or structure). Using the combination of deterministic modeling with the results of monitoring surveys and using a concept of separability, the author has developed a methodology for identifying the best model of the deformation mechanism from among several postulated models.

The Author's research has concentrated on:

- 1) optimal use of deterministic modeling in predicting structural and ground deformations in engineering, mining, and geoscience projects,
- 2) optimal combination (integration) of deterministic and geometrical models for the purpose of identifying the mechanism of deformation and explaining causes of the observed deformations,
- 3) optimal combination of deterministic models with observed deformations for the verification of material properties of the deformable body at the construction and post-construction (operation) stages,
- 4) propagation of variances-covariances in FEM,
- 5) modeling of gravity changes.

The research has concentrated on the analysis of large-scale problems using finite element analysis. The author developed a concept of equivalent (averaged) medium which may be divided into a few interacting blocks. The concept is used in forward and back analyses for studying the behavior of the rock mass. Since the properties of the in-situ rock may significantly differ from the results of the laboratory tests, methods for calibrating mechanical properties of rock or soil mass have been developed using a calibrating function, which is based on the distribution of compressive and tensional stresses. In addition, the author developed a methodology for the identification of material parameters of both brittle and salt (viscous) rock with application to mining problems and for soil structures with application to embankment dams.

The author has concentrated on the development of a methodology to model in-situ mechanical parameters for rock and for saturated soils. The scale ratio of laboratory Young modulus to in-situ Young modulus for intact rock is based on stress distribution in the rock mass. On the basis of stress distribution, the author also derived the scale ratio of a laboratory value of tensional strength to the in-situ values (SZOSTAK-CHRZANOWSKI and CHRZANOWSKI 1991). The assumptions regarding the behavior model of rock mass is used as a basis for the identification of boundaries of blocks within the rock mass with assigned to each block scaled parameters (CHRZANOWSKI et al. 2000).

In some cases of unexpected deformation of man-made or natural structures the causative factors may not be known. For example, the mechanism and causative factors of tectonic movements are usually not well known, and they are subjected to various hypotheses. The main purpose of the concept of integrated analysis developed by the author is to identify, on the basis of a comparison (or a simultaneous analysis) of geometrical and deterministic models, which of the postulated mechanisms can be optimally explained by the analysis. Depending on the design and accuracy of the monitoring surveys, the separation (discrimination) among various postulated mechanisms may not be possible (CHEN and CHRZANOWSKI 1986). In order to distinguish between these mechanisms, measurements of relative horizontal movements or gravity changes could help in the identification of the best model (SZOSTAK-CHRZANOWSKI et al. 1993a).

In this presentation examples are given on the applications of developed approach to modeling of deformations in:

- 1) determination of effects of mining and hydrological changes on ground subsidence in a potash mine PCS in Canada;
- 2) analysis of the deformations:
 - embankment dam West Dam of Diamond Valley Lake (DVL) Project in California,
 - embankment dam La Grande 4 main dam of La Grande Hydroelectric Complex located in northern Quebec, Canada, and

- Concrete Face Rockfill Dam (CFRD) Toulnustouc Main Dam located in northern Quebec, Canada;
- 3) studies of earth crustal movements in Western Canada;
- 4) error analysis of deformations in tunnel problem.

2. Modeling of ground subsidence in mining areas as a large – scale problem

Mining of a large deposit of high grade sylvinitite in New Brunswick has been carried out by Potash Corporation of Saskatchewan (PCS) since the mid 1980s (Fig. 1). Potash and salt mining at PCS takes place at depths between 400 m to 700 m within a 25 km long dome-shaped salt pillow in which the potash is preserved in steeply dipping flanks (Fig. 2). A strong, arch shaped, caprock provides an excellent natural support for the overlain brittle rocks. Potash is mined by using a mechanised cut-and-fill method with up to 100% extraction in the 1000 m long and about 150 m high stopes. Unsupported openings are up to 25 m wide. The potash deposit is structurally complex with a variable dip and width. Salt mining is by multi-level room-and-pillar method. Trans Canada Highway runs along the longitudinal axis of the mine and is affected by ground subsidence.

Annual monitoring of ground subsidence over the PCS mining operation near Sussex, N.B., has been carried out by the Canadian Centre for Geodetic



Fig. 1. PCS potash mine in New Brunswick Canada (Photo PCS)

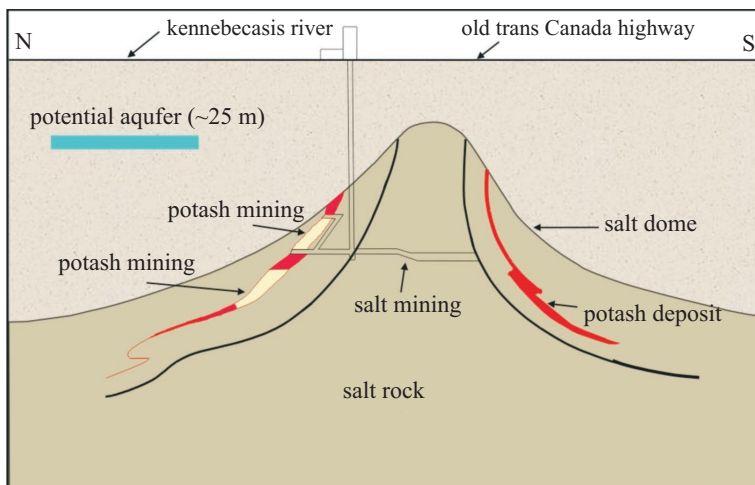


Fig. 2. Cross-section of the PCS potash and salt mine in New Brunswick

Engineering since 1989. Figure 2 shows the layout of the mining workings and the distribution of monitored points, which have been re-observed annually using levelling surveys, traversing of high precision with robotic total stations, and GPS measurements. In 1995, a finite element analysis was performed to model the maximum expected subsidence along a selected cross-section (line C-C in Fig. 3). A summary of the results was presented in (CHRZANOWSKI et al. 1998). The expected subsidence profile was to follow a regular shape with its maximum subsidence located above the room-and-pillar salt extraction (approximately above the centre of the salt dome).

Since 1997, a significant increase in water inflow to the mine was noticed at lower levels of potash extraction near the investigated cross-section and a secondary subsidence basin started occurring on the surface at the north end of the investigated cross-section along the C line of monitored points. Figure 4 shows development of ground subsidence along the C line of the monitored points between 1996 and 2003. Figure 3 shows the isolines of subsidence developed between 1996 and 2003 (CHRZANOWSKI and Szostak-CHRZANOWSKI 2004).

In 2003, a new FEM analysis of ground subsidence was undertaken to explain whether the water inflow from an unknown aquifer could cause the development of the secondary subsidence basin.

The following two basic models have been analysed:

- 1) analysis of ground subsidence as caused only by extraction of potash and salt,
- 2) analysis of ground subsidence as above, with an addition of possible effects of hydrological changes in the hypothetical aquifer (Fig. 2).

Due to a lack of information on the time dependent effects of mineral extraction and hydrological changes in the aquifer, the identification of the best

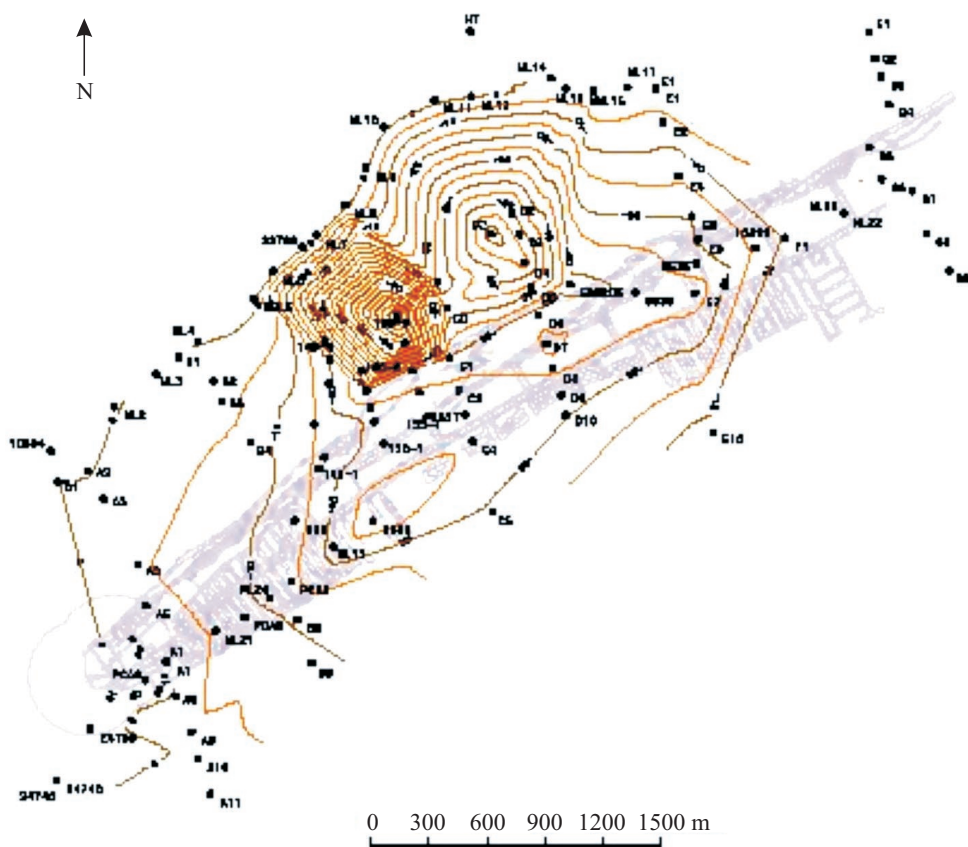


Fig. 3. Mine layout, monitoring points, and isolines of subsidence 1996-2003

model had to be based only on a qualitative analysis by comparing the shape of the FEM calculated subsidence profile with the observed subsidence curve.

In the first model only effects of salt and potash mining were investigated using FEM analysis. The analysis was performed for period 1996-2003. Figure 4 shows the FEM calculated profile of the surface subsidence along C-C line in comparison with the observed subsidence. The irregular observed subsidence could not be caused by the mineral extraction alone. Therefore, the second model with an effect of hydrological changes in the assumed aquifer was analyzed.

Three analyses were performed for assumed depths of the aquifer to be 350 m, 250 m, and 150 m. In each analysis, it was assumed that the centre of the aquifer is located under the point of the maximum subsidence (pt. C_0) of the secondary subsidence basin and that the compressibility value in the aquifer is such that the effect on the surface subsidence is approximately equal to the observed maximum subsidence of 0.46 m. The dimensions of the aquifer were arbitrarily taken as having the width of 330 m and thickness of 40 m. The

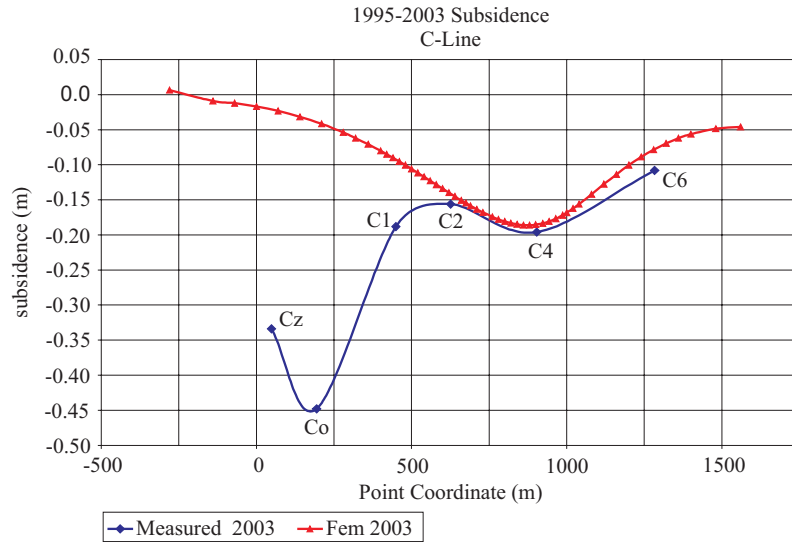


Fig. 4. Measured subsidence along C-C Line and calculated (FEM) subsidence due to only mineral extraction

analysis of the aquifer at the depth of 150 m gave the best agreement between the observed and modeled subsidence curve (Fig. 5). In 2003, in order to gain better information on the actual dimensions of the aquifer, the monitoring network was densified in the area of the expected aquifer.

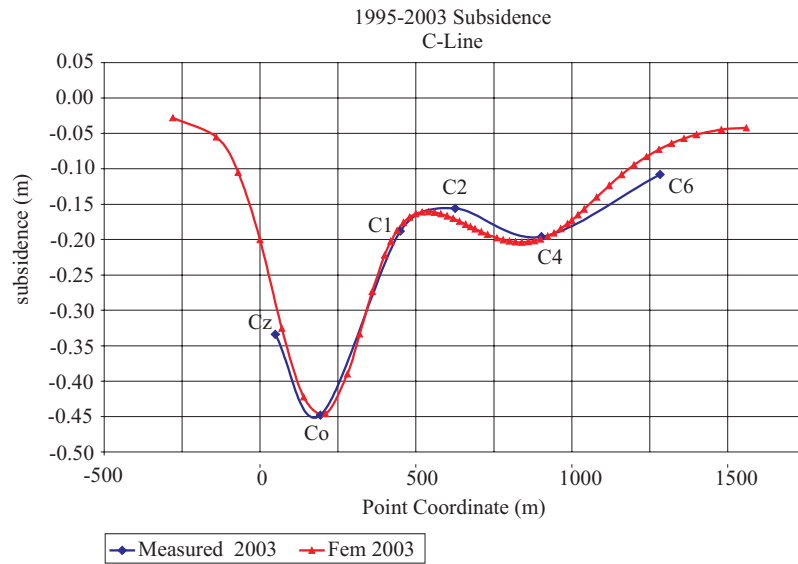


Fig. 5. Measured subsidence along C-C Line and calculated (FEM) subsidence with aquifer at 150 m depth

3. Modeling of subsidence due to withdrawal of oil in lagunillas oil field in venezuela

3.1. Characteristics of Lagunillas Oil Field

Venezuela has the western hemisphere's largest oil reserves of 77 billion barrels in four major sedimentary basins. There are three major oil fields: Tia Juana, Lagunillas, and Bachaquero extending from inland into the Lake Maracaibo. Among them, Lagunillas field is the largest with the total area of 163 km² and with over 1500 active wells (SZOSTAK-CHRZANOWSKI, CHRZANOWSKI, ORTIZ 2006). The area is divided into production blocks 1.4 km x 1.2 km (MURRIA 1991) containing 36 wells with one gathering station per block (FINOL and SANCEVIC 1997).

Data from the inland portion of Lagunillas has been selected for the preliminary testing of various methods for modeling ground subsidence. In Lagunillas oil fields oil is extracted from two, almost horizontal, reservoirs at two different levels: upper reservoir at the average depth $H_U = 674$ m and average thickness $h_U = 84$ m and lower reservoir at $H_L = 851$ m and $h_L = 37$ m. SZOSTAK-CHRZANOWSKI, CHRZANOWSKI, ORTIZ (2006) shows the outlines of the inland portion of the reservoirs. Monitoring of ground subsidence has been conducted on a bi-annual basis since 1926 using leveling of high precision (LEAL 1989). In 1988, GPS was added to the monitoring scheme to gain information on the horizontal movements (CHRZANOWSKI et al. 1988) and to connect the levelling network to far away reference points. The rate of subsidence in Lagunillas reaches 20 cm/y. In 2004, the maximum accumulated subsidence reached 7.0 m. In order to protect the inland part from flooding by the lake, a system of protective earth dykes is maintained and continuously upgraded (SZOSTAK-CHRZANOWSKI, CHRZANOWSKI, ORTIZ 2006, Fig. 1).

3.2. Available Data

A period of four years between 1996 and 2000 has been selected for the preliminary testing of deterministic modeling using finite element method (FEM). The following data has been obtained from PDVSA oil company to conduct the preliminary study:

- 1) results of bi-annual leveling,
- 2) CAD files showing boundaries, depth, and thickness of reservoirs,
- 3) locations of oil wells in the inland area
- 4) production history data for the inland area
- 5) observed pressures in individual oil wells (for upper and lower reservoirs).

In order to perform a preliminary analysis on the global correlation between production, change in pressure, compaction, and observed subsidence in the whole area, the data was averaged and generalized. It was more practical to perform a global study for the whole field rather than separate studies at each well. The compaction was assumed to be in soft clay layers in and adjoining the producing sand layers. Based on VAN DER KNAAP and VAN DER VLIS (1967), uniform compaction behavior over the area was assumed.

The productive area of the oil reservoir was identified based on the observed pressure changes (SZOSTAK-CHRZANOWSKI, CHRZANOWSKI, ORTIZ 2006, Fig. 2). To simplify the analysis, the upper and lower reservoirs in the productive area were combined into one reservoir of an average thickness of 240 m (SZOSTAK-CHRZANOWSKI, CHRZANOWSKI, ORTIZ 2006). The overburden material (unconsolidated sand) was accepted as homogenous and anisotropic. On the basis of the pressures observed in the wells, the productive area has been divided into two zones. The averaged pressure in Zone 1 was obtained as equal to -1000 kPa and in Zone 2 equal to -500 kPa (SZOSTAK-CHRZANOWSKI et al. 2006).

3.3. Modeling of subsidence using FEM

The preliminary two-dimensional FEM analysis was performed for the AA' cross-section shown in Figure 2; the geometry of the model followed Figure 3 (SZOSTAK-CHRZANOWSKI, CHRZANOWSKI, ORTIZ 2006). No tectonic stresses were included in the analysis, though it is known that the Lagunillas area is prone to

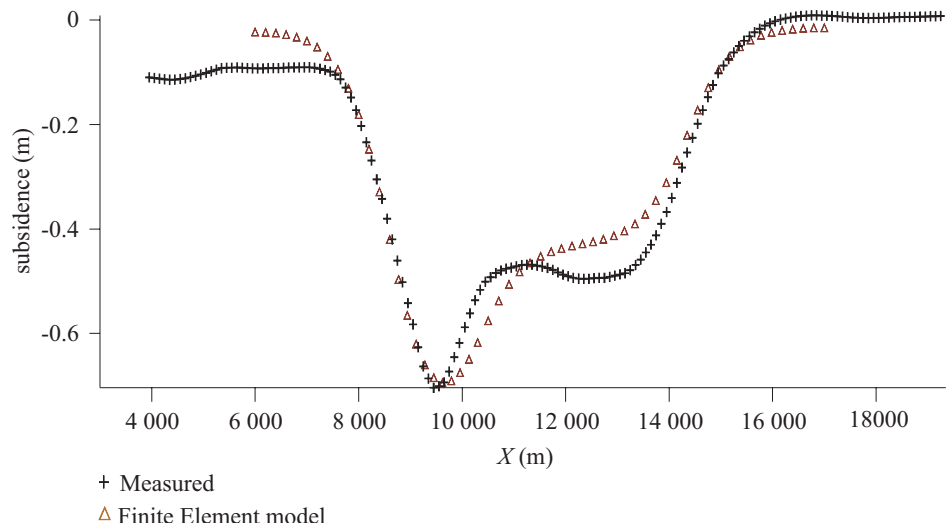


Fig. 6. Observed and modeled subsidence using FEM

seismic events. The given pressure changes in the oil wells were used as the loading condition. The value of Poisson ratio was taken as $\nu = 0.3$, while the value of Young modulus was obtained through calibration by taking the calculated subsidence at the point of maximum subsidence equal to the observed value and was assumed as $E = 183$ MPa. Figure 6 shows comparison between the observed and modeled subsidence using FEM

4. Integrated analysis of earth and rockfill dams

4.1. Purpose of integrated analysis of earth and rockfill dams

Safety of earth dams depends on the proper design, construction, and monitoring of actual behaviour during the construction and during the operation of the structure. In the design of the earth dams, the finite element method (FEM) is used very often. The FEM is used in the analyses of expected displacements, strains, and stresses in the structure caused by changeable loading or boundary conditions. The values calculated from FEM may be compared with measured values during construction and filling up a reservoir giving additional information on the actual behaviour of the structure, boundary conditions and unexpected loads.

The geotechnical parameters of the earth material play significant role in the stability of the dam. The dams located in the seismically stable areas are built with the material characterized by such geotechnical parameters which allows for a dam to be more adaptable to the changes. The behaviour of the earth material may be determined using hyperbolic non-linear model (KONDNER 1963) and (KONDNER and ZELASKO 1963). In this presentation the author gives examples of the predicted deformations for various earth dams and discusses the effect of the prediction results on the proper design of the monitoring surveys.

4.2. Diamond Valley Lake Project

Recently completed Diamond Valley Lake (DVL) project (Fig. 7), consists of three dams (ARITA et al. 2000). The DVL dams have been constructed from soil and rock. Figure 7 shows a typical cross-section of the West Dam with height of 87 m. The area of the DVL is located within the interaction zone between the North American and Pacific tectonic plates. The San Jacinto and San Andreas faults are located about 10 km and 30 km, respectively, from the reservoir. Therefore, in designing the dam deformation monitoring surveys one had to consider not only loading effects of the reservoir and gravitational settlement of the dams but also effects of earth crust movements in this



Fig. 7. Diamond Valley Lake project

seismically active area that is prone to frequent earthquakes. The local monitoring network was connected to the existing GPS regional network of the continuously operating reference stations (CORS) of Southern California (BOCK et al. 1997) which monitor the earth crust movements.

A fully automated monitoring scheme with a telemetric data acquisition was designed using both geotechnical and geodetic instrumentation (DUFFY et al. 2001). Geotechnical instrumentation was designed independently of the geodetic portion of the monitoring plan. It includes a total of 262 piezometers, 7 inclinometers, 74 settlement sensors, 6 fixed embankment extensometers, 14 weirs and 18 strong motion accelerographs. The automated geodetic monitoring system consists of 8 robotic total stations (Leica TCA1800) with the automatic target recognition and electronic measurements of angles and distances. In addition, 5 continuously working GPS receivers were permanently installed on the crests of the dams to provide a warning system that “wake up” the robotic total

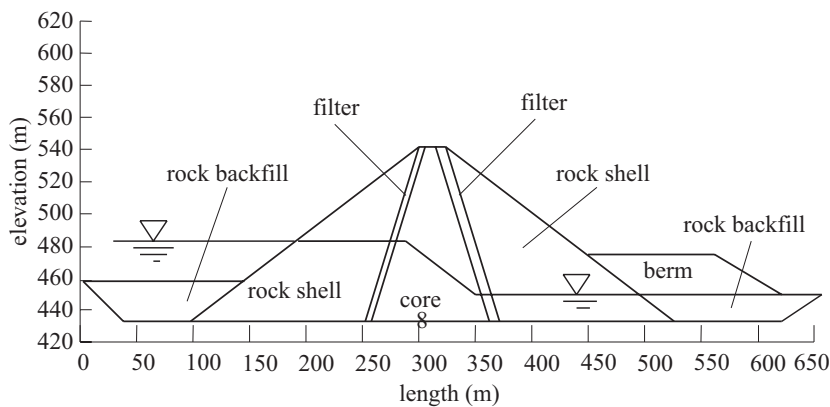


Fig. 8. Schematic cross-section of the West Dam with dry and wet zones

stations in case of abnormally large displacements. The accuracy of the geodetic measurements was designed to detect displacements larger than 10 mm at 95% confidence level (WHITAKER et al. 1999).

The DVL dams have been constructed from soil and rock. The core materials are silty and clayey sandy alluviums obtained from the floor of the reservoir and the rock fill was obtained from bedrock hills of the reservoir. Figure 8 shows as a typical cross-section of the West Dam. Table 1 lists geotechnical parameters used in the analysis of West Dam.

In Table 1, ϕ is an angle of friction, γ is unit weight, K is loading modulus number, n is exponent for loading behaviour, K_b is bulk modulus number, m is bulk modulus exponent, K_o is the earth's pressure ratio, and R_f is the failure ratio. The wet parameters are smaller than dry parameters for the same soil.

Table 1

Geotechnical Parameters for the DVL Dam

Parameters	Core	Filters	Rockfill shell
γ (kN/m ³)	22	20.42	22
ϕ	38°	47°	45°
K_o	0.5	0.5	0.5
K	500	560	560
K_b	210	330	330
n	0.55	0.48	0.48
m	0.4	0.33	0.33
R_f	0.7	0.65	0.65

The wet parameters were obtained using the relations shown in Table 2 for filter and shell (TOUILÉB et al. 2000). For core, the wet parameters are given for the 0 m, 20 m, 40 m, 60 m, and 80 m height of water at the West Dam in Table 3 (MASSIERA et al. 2004). The schematic cross-section of the West Dam with dry and wet zones is given on Figure 9.

Table 2

Geotechnical parameters for saturated conditions at West Dam

Zone	K_{sat}	$K_b \text{ sat}$
Filter	$K_{\text{sat}} = 0.85 K = 476$	$K_b \text{ sat} = 0.85 K_b = 280.5$
Rockfill shell	$K_{\text{sat}} = 0.60 K = 336$	$K_b \text{ sat} = 0.60 K_b = 198.0$

Table 3

Geotechnical parameters for core in saturated conditions as a function of the height of the water at the West Dam

Height of water (m)	K_{sat}	$K_b \text{ sat}$
0	$K_{\text{sat}} = 0.9 K = 450$	$K_b \text{ sat} = 0.9 K_b = 189$
20	$K_{\text{sat}} = 0.8 K = 400$	$K_b \text{ sat} = 0.8 K_b = 168$
40	$K_{\text{sat}} = 0.8 K = 400$	$K_b \text{ sat} = 0.8 K_b = 168$
60	$K_{\text{sat}} = 0.7 K = 350$	$K_b \text{ sat} = 0.7 K_b = 147$
80	$K_{\text{sat}} = 0.6 K = 300$	$K_b \text{ sat} = 0.6 K_b = 126$

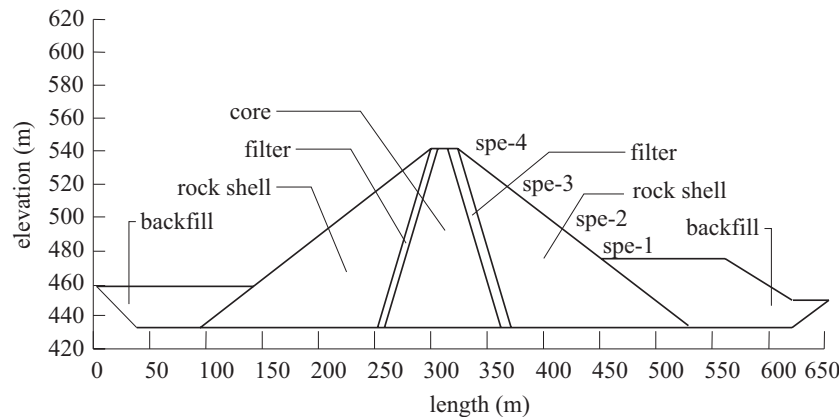


Fig. 9. Schematic cross-section of the West Dam

4.3. La Grande 4 (LG-4) Project

La Grande 4 (LG-4) main dam is the second largest structure of the La Grande Complex (LGC) of James Bay hydroelectric development located in northern Quebec, (PARÉ et al. 1984). LG-4 main dam has maximum height of 125 m and is 3.8 km long. LG-4 main dam is a zoned embankment. The dam is constructed almost entirely on bedrock. During the construction of the La Grande Complex, the main installed instruments were: inclinometers with tubes with telescopic joints, settlement cells, and linear extensometers, surface movements, hydraulic and electrical piezometers, electrical vibrating wire and pneumatic total pressure cells, and weirs (VERMA et al. 1985). It allowed following behaviour of the embankment during the construction and during the filling up the reservoir. The geotechnical parameters are given in Table 4 (MASSIERA et al. 2003).

Table 4

Geotechnical parameters (LG-4)

Parameters	Core	Filters and transition	Shell
K	1670	4500	1000
K_b	1030	2850	(300)
n			800
m	0.5	0.4	0.8
R_f	0.5	0.4	0.8
ϕ	0.5	0.6	0.35
K_o	37°	42°	45°
γ	0.35 21.44	0.33 22.60	0.29 19.62

4.4. Concrete Face Rockfill Dam (CFRD): Toulnustouc Main Dam

The Toulnustouc main dam is located north of the city of Baie-Comeau on the Toulnustouc River in Northern Quebec (Fig. 10). The existing dam has 75 m height and is 0.575 km long and it is built on bedrock foundation. The thickness of the concrete face slabs is 0,3 m. Instrumentation installed in the structure included 13 submersible tilt meters, 1 measuring wire, 22 fissurometes (crack meters), 2 accelerometers, one measuring weir, and 16 survey markers.

There was a long-term monitoring of slab deflection, which is caused by the dominant hydrostatic load moving the concrete face gradually in the downstream direction. Each instrument had to withstand a maximum of 75 m head of water



Fig. 10. Toulnustouc (CFRD) main dam (<http://www.waterpowermagazine.com/home.asp>)

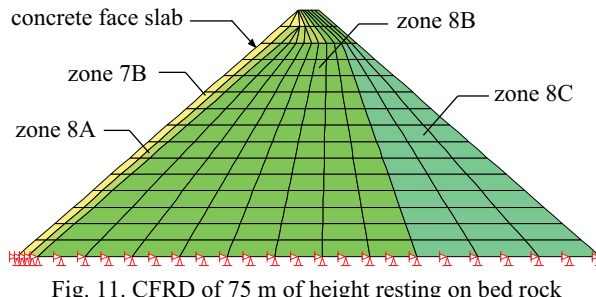


Fig. 11. CFRD of 75 m of height resting on bed rock

and be sufficiently accurate to measure small deformations (mm scale). The analyzed cross-section of the dam is shown on Figure 11.

The values of the geotechnical parameters used in the analysis of the Toulnustouc main dam are presented in Table 5 (RSW INC 2001). The following zones are specified: zone of the crushed stone with maximum grain size 80 mm (zone 7B), zone of the crushed stone with maximum grain size 200 mm (zone 8A), rockfill with maximum grain size 900 mm (zone 8B), and zone of rockfill with maximum grain size 1800 mm (zone 8C).

Table 5

Values of geotechnical parameters

Parameters	Rockfill Zones 7B and 8A	Rockfill Zone 8B	Rockfill Zone 8C	Foundation of Till (Moraine)	Foundation of granular alluviums		
					0-30 m	30-60 m	>60 m
K	1000	500	400	1670	800	1000	1200
K_b	800	240	240	1030	400	500	600
n	0.5	0.5	0.5	0.5	0.5	0.5	0.5
m	0.2	0.2	0.2	0.5	0.2	0.2	0.2
R_f	0.35	0.35	0.35	0.5	0.7	0.7	0.7
K_{ur}	1200	600	480	2004	0	0	0
ϕ	45°	45°	45°	37°	32°	32°	32°
γ (KN/m ³)	19.5	19.5	19.5	21.44	18.8	19.0	19.5

4.5. Geotechnical Parameters of the Earth and Rock Fill

The geotechnical parameters used in the design of DVL dams differ quite significantly from the parameters used in LGC project (SZOSTAK-CHRZANOWSKI et al. 2000). Loading modulus number K and bulk modulus number K_b for LGB dam are larger than for DVL dam. The exponent for loading behaviour n and modulus exponent m for LGB dam are larger than for DVL dam.

4.6. Summary of Deformations Analysis using FEM

The presented three cases of dams were analysed using finite element method and SIGMA/W software (KRAHN 2004). The behavior of the earth/rockfill dams was analyzed in two stages. First stage was an analysis of the behavior during construction of a dam. The second stage was an analysis of a response of the constructed structure to the filling of the reservoir with water. The analysis of settlements during construction of LG4 main dam was performed for two assumed heights: 84 m and 120 m. The dam was assumed to rest on non-deformable bedrock. The analysis of DVL dam was performed for West Dam with the assumption that the dam was resting on non-deformable bedrock. Two models of CFRD-Toulnustouc main dam were analysed. The first model of the dam followed the real foundation conditions and the dam was resting on bedrock foundation. The second model was a simulation of the dam structure resting on a 60 m high foundation of dense till (moraine).

The calculated settlements in the center during the construction are much larger for DVL dam than for LG4 main dam. The maximum settlement in the center of West Dam (height 88 m) is 0.23 m and is located at the 54 m elevation. For the LG4 dam (height 84 m) the maximum settlement in the center of the dam is 0.12 m and is located at 36 m elevation (Fig. 12). The calculated horizontal displacements of West Dam using DVL parameters are larger than using LGC parameters.

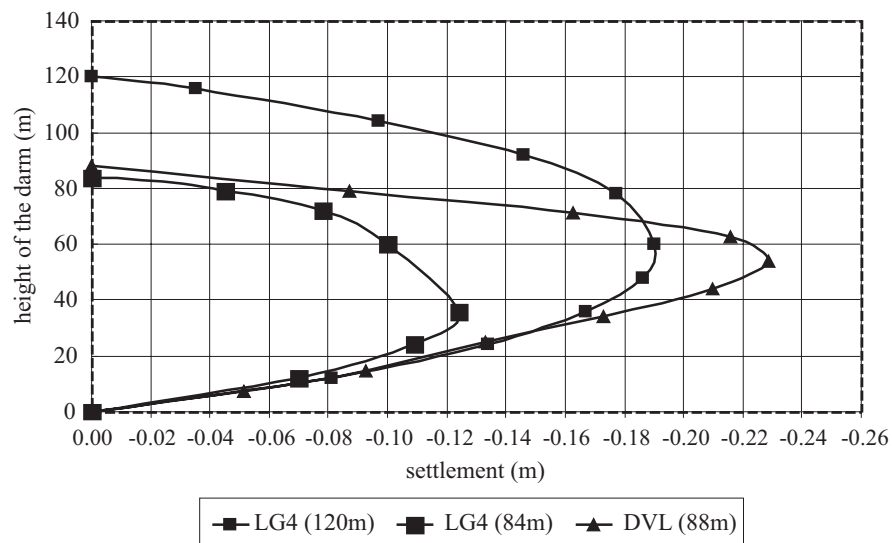


Fig. 12. The calculated settlements at the end of construction of DVL and LGC dams

The comparison of vertical displacements at the crest of West Dam and CFRD Toulnustouc main dam during the filling of reservoir with water are shown on Figure 13. The West Dam has larger vertical displacements of crest at the end of filling the reservoir. The deformation rates are also different for each case. As one can see from the comparison of predicted rates of the displacements expected at DVL dam and CFRD dam, the DVL dam will require more frequent observations because of the larger acceleration of the movements than in the case of CFRD dam.

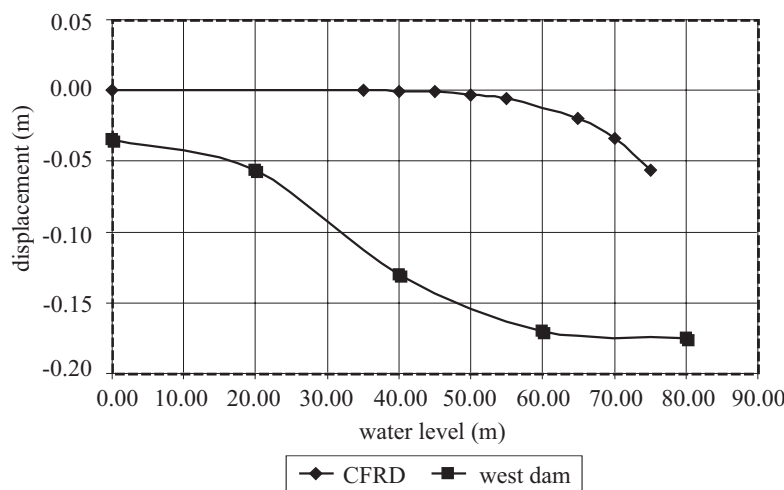


Fig. 13. Vertical displacement of crest during filing up a reservoir

In case of the CFRD dam, the maximum displacements are expected to occur on upstream face of the dam, where classical geodetic surveys cannot be implemented (see Fig. 11). Thus, in this case permanently installed geotechnical instruments (e.g., inclinometers, extensometers) should be used on the upstream face while geodetic surveys could be utilized on the crest and the downstream face. Here one should note that the maximum displacements of the upstream (concrete) face are expected to take place 40 metres below the crest and is reaching 0.22 m for the dam resting on bedrock. This is very often overlooked by geodetic engineers, who tend to install their points along the crest due to the easiest access. The maximum displacements of the concrete face slab were function also of the height of the dam during the filling of the reservoir. The calculated settlements for CFRD dam at the end of filling up a reservoir are shown on Figure 14. The displacements are larger when the dam is resting on 60 m of till (Fig. 14). The magnitude of horizontal displacements is larger than magnitude of settlements. The calculated horizontal displacements are larger for CFRD resting on bedrock (Fig. 15).

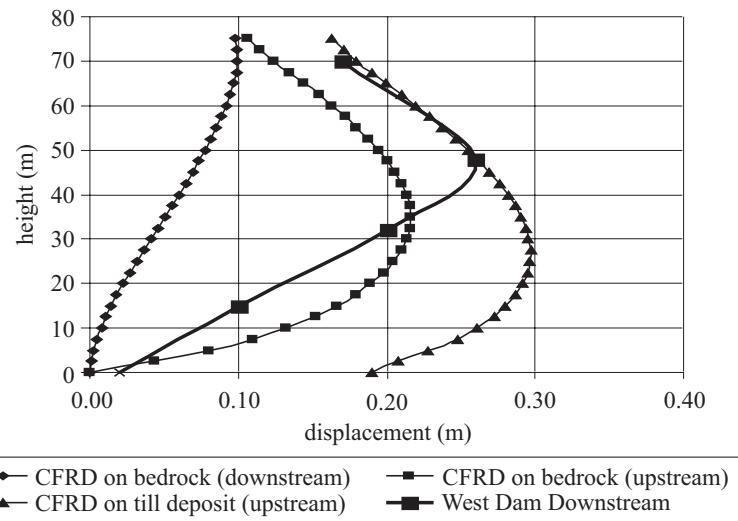


Fig. 14. Displacements of CFRD and West Dam at the end of filling up a reservoir

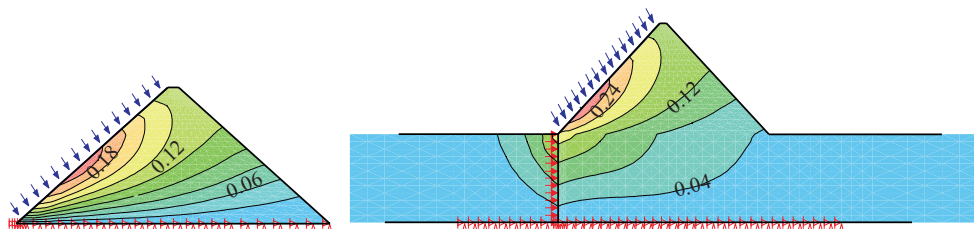


Fig. 15. Calculated horizontal displacements (m) at the end of the filling of the reservoir

5. Numerical modeling of gravity changes of tectonic origin

5.1. Preliminary remarks

Relocation of rock masses and/or change of density, and change of height due to human (e.g., mining) activities or tectonic activity may produce significant local changes to the gravity field in the vicinity of activity. The gravity changes result in local tilts of the level surface (equipotential surface of gravity) and, consequently, changes of the direction of the plumblines to which the majority of geodetic and some geotechnical measurements are referenced. Thus, if any geodetic measurements of high precision are required during the mining operation, for example, for the purpose of monitoring the stability of surface structures, they should be corrected for changes of gravity and deflection of the vertical as a function of time. The method has been used in modeling regional deformations

and gravity changes of tectonic origin (SZOSTAK-CHRZANOWSKI et al. 1996) and in modeling expected gravity changes in a large open pit mine, Belchatow, in Poland (SZOSTAK-CHRZANOWSKI et al. 1995).

5.2. Geometry and physical properties of the investigated models

The author investigated the gravity changes caused by tectonic activity. Following three models of tectonic movements and their effects on the surface deformation and gravity changes have been investigated:

- a) influence of a deeply located dilating sphere (e.g. magma intrusion and/or thermal expansion),
- b) influence of a slightly dipping thrust fault locked to a certain depth below the surface, and
- c) influence of a dislocation along a vertical fault locked to a certain depth below the surface.

The models (a) and (b) were thoroughly investigated by RUNDLE (1978) who tried to solve analytically the determination of the surface uplift and gravity changes due to the above causative effects. Although the geometry of the models is very simple, the analytical solutions required extensive approximations and simplifications regarding the properties of the material (rocks). Detailed results of a comparison between Rundle's and the authors' solutions for various material properties in models (a) and (b) have been given in SZOSTAK-CHRZANOWSKI (1992). This paper summarizes only FEM solutions in order to draw conclusions on the usefulness of gravity measurements in solving the problem of the separability of deformation models.

As an example, the following three models of tectonic movements and their effects on surface deformation have been investigated using FEM software package FEMMA (SZOSTAK-CHRZANOWSKI et al. 1993a):

MODEL A: Influence of a deeply located dilating sphere. The dilating sphere with a radius of 15 km is centred 30 km below the surface (Fig. 16). It was assumed that the expansion of the sphere was produced either by a uniform hydrostatic pressure or by thermal stresses.

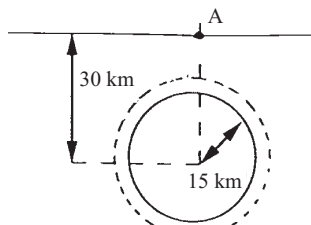


Fig. 16. Geometry of the sphere (model A)

MODEL B: Influence of a slightly dipping thrust fault. The thrust fault (Fig. 17) with a dip angle of 10° was assumed to be locked at a depth of 20 km where the open portion of the fault exhibits slip in two opposite directions along the fault plane over a distance of 200 km.

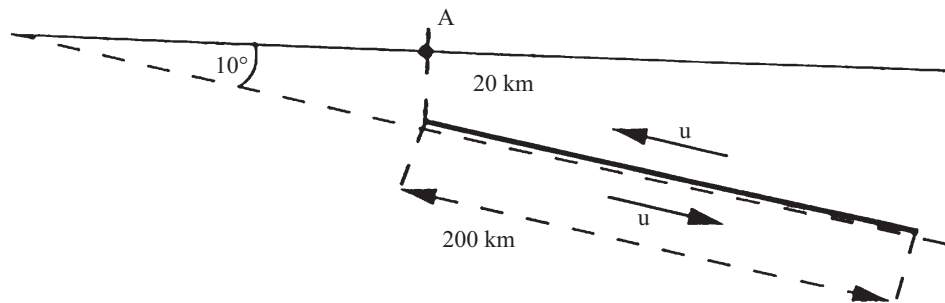


Fig. 17. Geometry of the thrust fault (model B)

MODEL C: Influence of a dislocation along a vertical fault (Fig. 18). The vertical fault was also assumed to be locked at a depth of 20 km and slipping along the fault plane in two opposite directions.

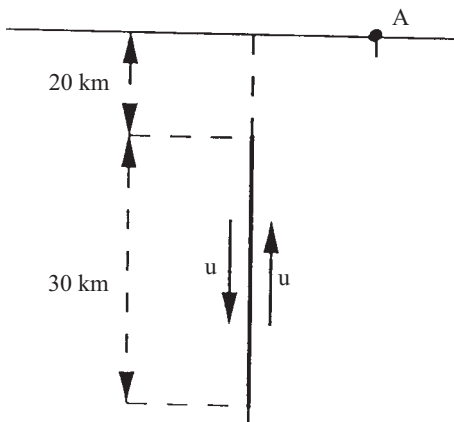


Fig. 18. Geometry of the vertical fault (model C)

In all three models, the rock strata was assumed to be homogeneous, linear-elastic, and isotropic with the Young modules $E = 10^{11}$ Pa and the Poisson ratio $\nu = 0.25$. In models B and C, the width of the faults in the vertical cross section was taken as equal to 0.1 km. In order to make the surface deformation effects of all three tectonic models compatible, the boundary conditions for the FEM analysis were selected so that the surface uplift of point '0' would be the same in each model and equal to 0.25 m. It was calculated that in order to obtain the

uplift of 0.25 m produced by the dilating sphere, the expansive body forces per unit volume would have to be equal to $f = 1831.5 \times 10^9 \text{ N/km}^3$.

5.3. Effects of the Dilating Sphere

The FEM model was defined in x , y , z coordinate system. Since the geometry of the sphere is symmetrical, only one fourth of the sphere has been modelled in the 3-D finite element analysis. The following displacement boundary conditions were accepted: the lower xz plane was fixed, the upper xz plane was free, the left yz plane was constrained in x direction, the right yz plane was constrained in x direction, the xy planes (front and back) were constrained in z direction, and the nodal points located on the cross section of the planes were constrained by adding the constraints of the planes. An assumption was made that the mass of the dilating sphere remained constant. Using software FEMMA, it was calculated that in order to obtain the uplift of 0.25 m produced by the dilating sphere, the expansive body forces per unit volume would have to be equal to $f = 1831.5 \times 10^9 \text{ N/km}^3$. Using the above expansive body forces and the boundary conditions, the vertical and horizontal displacements on the surface could be calculated. Figures 19 and 20 show the calculated uplifts and horizontal displacements at nodal points on the surface. Figure 21 shows the calculated gravity changes.

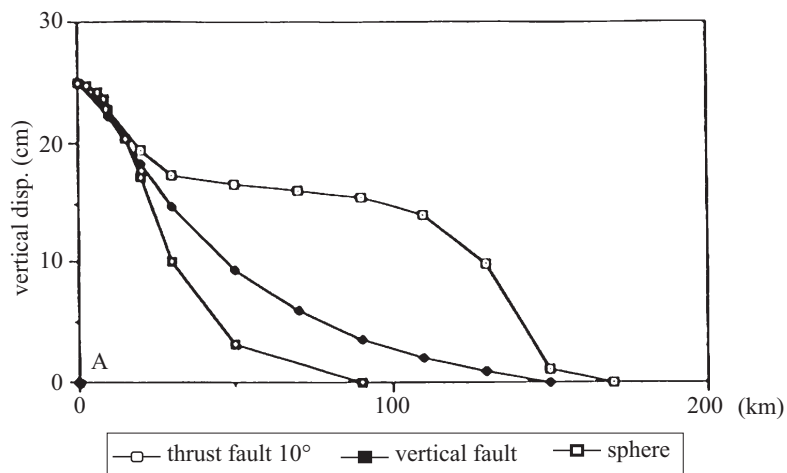


Fig. 19. Vertical displacements

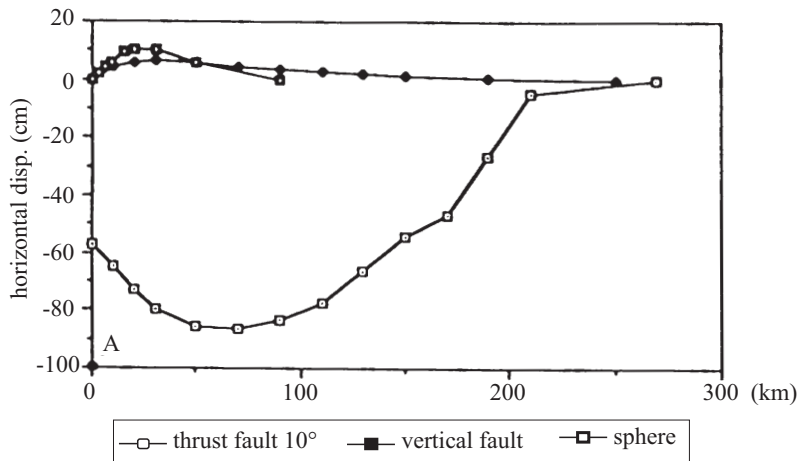


Fig. 20. Horizontal displacements

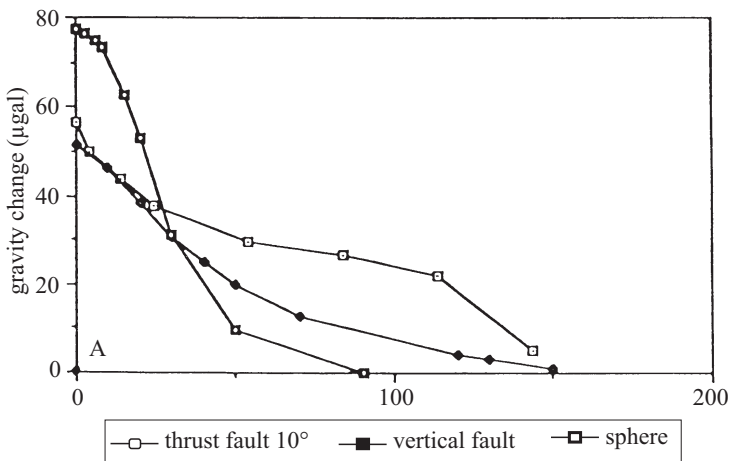


Fig. 21. Gravity change

5.4. Effects of the Faults

Figure 17 and Figure 18 shows the geometry of the effects of dislocations along the slightly inclined thrust fault and along the vertical fault. It was calculated that in order to satisfy the condition that point '0' on the surface should be uplifted 0.25 m, the values of the dislocations u had to be:

- 1) for the thrust fault, $u = 98.5$ cm,
- 2) for the vertical fault, $u = 57$ cm.

These values were introduced into the FEM analysis as upward and downward displacements (total relative displacements of $2 u$) of nodal points along the opposite surfaces of the active fault zone. Figures 19 and 20 summarize the results of the calculated displacements on the surface. Figure 21 shows the calculated gravity changes.

5.5. Discussion of the Results of Modeling

The results shown in Figure 19 indicate that geodetic levelling alone could not discriminate between the effects of the sphere and the vertical fault, particularly if the maximum uplift of pt. A would be smaller than the value of 25 cm. However, the separation in vertical displacements caused by the vertical or by the thrust fault dislocations is large enough to be detected by geodetic levelling.

Similarly, the results of the horizontal displacements (Fig. 20) show that the effects of the sphere and the vertical fault are practically the same, i.e., that measurements of horizontal displacements or horizontal components of strain could not discriminate between the two tectonic effects. However, the effect of the thrust fault is distinctly different than the effects of the two other models.

The results of gravity changes (Fig. 21), indicate that, perhaps, the model of the expanding sphere could be separated from the effects of other two models if the gravity surveys were performed in the vicinity of point A. At larger distances (say, 100 km) from point A, the effects of the thrust fault could, perhaps, be separated from the other effects.

Generally, the presented methodology based on the finite element analysis and use of FEMMA shows the potential of its implementation in practice in designing the monitoring surveys according to the postulated tectonic models. One should remember, that the given examples were calculated for a rather large assumed uplift of 25 cm at point A. If the actual uplift was ten times smaller (i.e., 25 mm), the maximum difference in the gravity changes for the three models would be only 2 mgal, which would be beyond the actual accuracy of the field gravimeters.

6. Propagations of errors in forward and back analyses using fem

6.1. Forward analysis of a tunnel problem

Results of any measurements (treated as random variables) or quantities derived from random variables are meaningless unless they are accompanied by information on their accuracy. The example shows a practical application of the methodology for the error propagation in a tunnel excavated at a depth of 30 m in homogeneous rock (one type of material only). A linear elastic FEM analysis was performed using the aforementioned software FEMMA to calculate expected displacements at the nodal points of the FEM mesh resulting from the excavation of the tunnel (SZOSTAK-CHRZANOWSKI et al. 1993b). The following rock properties have been assumed:

Young modulus: $E = 1000 \text{ MPa}$ with the error $\sigma_E = 100 \text{ MPa}$,

Poisson ratio: $\nu = 0.25$ with the error $\sigma_\nu = 0.025$,

Unit weight: $\gamma = 19 \text{ KN/m}^3$ (errorless).

The weight of the rocks was taken as the only load (body forces) producing the displacements due to the excavation.

The calculated using FEM displacements at several selected points on the surface and in the tunnel and their standard deviations, obtained from the propagation of the random errors, are listed in Table 6.

T a b l e 6

The predicted displacements and their corresponding standard deviations

Point	dx (mm)	σ_{dx} (mm)	dz (mm)	σ_{dz} (mm)
p1	0.08	0.05	-0.12	0.14
p2	0.00	0.00	-0.21	0.19
p3	0.00	0.00	-1.40	0.60
p4	0.44	0.90	-0.14	0.12
p5	0.00	0.00	1.13	0.51

The points 1, 2, 3, 4, and 5 locations were selected as:
 point 1 is located on the surface 5 m of the center of the tunnel,
 point 2 is located on the surface over the center of the tunnel,
 point 3 is located in the center of the top of the tunnel opening,
 point 4 is in the center of the wall of the tunnel opening, and
 point 5 is located in the center of the floor of the tunnel.

6.2. Back analysis

In order to illustrate the application of the error propagation in the back analyses, it was assumed that in the above example the value of Young Modulus E for the rock was unknown and it was supposed to be determined in-situ through the back analysis from observed vertical displacements at some selected points.

In the back analysis three cases were considered:

- case #1 when the observations are made only at pt. 2,
- case #2 with observations only at pt. 3,
- case #3 when displacements at points 1, 2, 3, 4, and 5 are observed.

The values of the observed vertical displacements were taken as listed in Table 6. It was assumed that the vertical displacement of each point had been obtained from repeated geodetic levelling of high precision with standard deviations of 0.5 mm. Table 7 lists the expected errors (standard deviations) of Young Modulus as obtained from individual vertical displacements and when all

Table 7

Young modulus E and its accuracy (sE) calculated from the measured vertical displacements

Point	dz (mm)	σ_{dz} (mm)	E (MPa)	σ_E (MPa)
p1	3.13	0.50	999.6	79.7
p2	1.43	0.50	999.7	127.4
p3	-0.44	0.50	999.4	568.4
p4	-2.78	0.50	999.8	64.6
p5	-3.87	0.50	999.8	89.9

five displacements were observed. The results show that, as it could have been expected, the weakest determination of Young Modulus E was obtained when measurements of the vertical displacements were limited to only point 2 (Table 8). The observations limited to only point 3 gave the value of Young Modulus with an error only slightly larger than in Case #3, i.e. when observations of the displacements were made at all five points.

Table 8

Accuracy of E calculated from the observed vertical displacements

Case:	#1 (pt. 2)	#2 (pt. 3)	#3 (pts. 1, 2, 3, 4, and 5)
σ_E (MPa):	1860	285	220

The described methodology provides a tool for the rigorous propagation of variances and covariances in the finite element modeling of deformations and in the finite element back analyses when properties of the material and/or boundary conditions are supposed to be determined from observed deformations of a known accuracy. Although the given examples deal only with a homogeneous and linear elastic material, the method can be used in more complex FEM analyses.

7. General conclusions

The given examples illustrate practical applications of the author's developments in the interdisciplinary approach to deformation analysis. The combination of monitoring results with deterministic modeling provide a powerful tool in the determination of the deformation mechanism and in the verification of material properties of the investigated object.

Acknowledgements

This research was made with the financial support of the Natural Science and Engineering Research Council of Canada, Atlantic Innovation Fund, ACA Ltd., and the Faculté des Études Supérieures et de la Recherche de l'Université de Moncton. Prof. A. Chrzanowski and Prof. M. Massiera collaborated in this research.

References

- ARITA A.A., FORREST M.P., FOTHERINGHAM J.R., MAJORS D.G. 2000. *Three dams, one reservoir*. American Society of Civil Engineers, 70: 28-31.
- BOCK Y., WDOWINSKI S., FANG P., ZHANG J., BEHR J., GENRICH J., WILLIAMS S., AGNEW D., WYATT F., JOHNSON H., STARK K., ORAL B., HUDNUT K., DINARDO S., YOUNG W., JACKSON D., GURTNE W. 1997. *Southern California Permanent GPS Geodetic Array: Continuous Measurements of Regional Crustal Deformation between the 1992 Landers and 1994 Northridge Earthquakes*. J. Geophysical Research, 102 #B8: pp. 18013-18033.
- CHEN Y.Q., CHRZANOWSKI A. 1986. *An overview of the physical interpretation of deformation measurements*. Deformation Measurements Workshop, MIT, Boston, Oct. 31-Nov. 1, Proceedings (MIT): 207-220.
- CHRZANOWSKI A., CHEN Y.Q., LEEMAN R., LEAL J. 1988. *Integration of the Global Positioning System with geodetic leveling surveys in ground subsidence studies*. Proceedings 5th International (FIG) Symposium on Deformation Measurements, UNB, Fredericton, N.B., Canada: pp. 142-151.
- CHRZANOWSKI A., SZOSTAK-CHRZANOWSKI A., FORRESTER D.J. 1998. *100 Years of ground Subsidence*

- Studies.* 100th General Meeting of CIM, Montreal, May 3-7, Proceedings (anadiaCn Institute of Mining) – CD-ROM, CIM Montreal '98.
- CHRZANOWSKI, A., SZOSTAK-CHRZANOWSKI A., BASTIN G., LUTES J. 2000. *Monitoring and Modeling of Ground Subsidence in Mining Areas-Case Studies.* Geomatica: pp. 405-413.
- CHRZANOWSKI A., SZOSTAK-CHRZANOWSKI A. 2004. *Physical Interpretation of Ground Subsidence Surveys – A Case Study.* Journal of Geospatial Engineering, Hong Kong Institute of Engineering Surveyors: pp. 21-29.
- DUFFY M., HILL C., WHITAKER C., CHRZANOWSKI A., LUTES J., BASTIN G. 2001. *An automated and integrated monitoring program for Diamond Valley Lake in California.* Proceedings (CD Rom) 10th Int. Symp. on Deformation Measurements (Metropolitan Water District of S. California), Orange, CA, March 19-22: pp. K-1 to K-8. Available at: <http://rincon.gps.caltech.edu/FIG10sym/>.
- FINOL A.S., SANCEVIC Z.A. 1997. *Subsidence in Venezuela.* Subsidence due to Fluid Withdrawal. Edd. Chilingarian G. V., E. C. Donaldson, and T.F. Yen, Elsevier Science, Development in Petroleum Science, 41, Ch-7: 337-372.
- KONDNER R.L. 1963. *Hyperbolic stress-strain response: cohesive soils.* Journal of the Soil Mechanics and Foundation Division, ASCE, 89 (SM1): 115-143.
- KONDNER R.L., ZELASKO J.S. 1963. *A hyperbolic stress-strain formulation of sand.* Proceedings of the 2nd Pan American CSMFE, Brazil, 1: 289-324.
- KRAHN J. 2004. *Stress and deformation modeling with SIGMA/W, an engineering methodology.* GEO-SLOPE International Ltd., Calgary, Alberta.
- LEAL J. 1989. *Integration of GPS and leveling in subsidence monitoring studies at the Costa Bolivar oil fields.* Technical Report No. 144. Dept. Of Surveying Engineering, University of New Brunswick, Fredericton, N.B., Canada.
- MASSIÉRA M., SZOSTAK-CHRZANOWSKI A. 2003. *Contraintes et déformations dans les barrages zonés en remblai lors de leur construction.* Proceedings, 56-th Annual Canadian Geotechnical Conference, Winnipeg, CD Rom, Session 2B, 8p.
- MASSIÉRA M., CORMIER A., HAMMAMI Y., SZOSTAK-CHRZANOWSKI A. 2004. *Prévisions des déformations et contraintes dans les barrages en enrochement avec masque amont en béton.* Proceedings, 57-th Annual Canadian Geotechnical Conference, Québec, CD Rom, Session, 5F: 9-16.
- MURRIA J. 1991. *Subsidence in Western Venezuela Oil Fileds – Subsidence and Prediction.* Proceedings VIIth Intern. Congress of the Int. Soc. For Mine Surveyors, Lexington, USA, Sept. 22-27: 439-443.
- PARÉ J.J., VERMA N.S., KEIRA H.M.S., McCONNELL A.D. 1984. *Stress-deformation prediction for the LG-4 main dam.* Canadian Geotechnical Journal, 21(2): 213-222.
- RSW Inc. 2001. *Aménagement de la Toulnustouc, Barrage-variante as masque amont.* Resultat de l'analyse contrainte-déformation. Rapport, 11 p.
- RUNDLE J. 1978. *Gravity changes and the Palmdale Uplift.* Geophysical Research Letters, 5(1): 41-44.
- SZOSTAK-CHRZANOWSKI A., CHRZANOWSKI A. 1991a. *Modeling and Prediction of Ground Subsidence using an Iterative Finite Element Method.* Proceedings 4-th International Symposium on Land Subsidence, Ed. A. I. Johnson, Houston, Texas, 12-17 May, International Association of Hydrological Sciences, Publication, 200: 173-180.
- SZOSTAK-CHRZANOWSKI A. 1992. *Height and Surface Gravity Effects from Dilating Spherical Cavity and Thrust Fault.* Final Report, EMR, Geophysics Division Contract, September.
- SZOSTAK-CHRZANOWSKI A., CHRZANOWSKI A., LAMBERT A., PAUL M.K. 1993a. *Finite Element Analysis of Surface Uplift and Gravity Changes of Tectonic Origin.* Proceedings 7-th International FIG Symposium on Deformation Measurements, 6-th Canadian Symposium on Mining Surveying, Banff, Alberta, (ed. W. F. Teskey), 3-5 May, 333-341.

- SZOSTAK-CHRZANOWSKI A., CHRZANOWSKI A., KUANG S. 1993b. *Propagation of Random Errors in Finite Element Analyses*. Proceedings 1-st Canadian Symposium on Numerical Modeling Applications in Mining and Geomechanics, (ed. H. Mitri), Montreal, PQ., 27-30 March, 297-307.
- SZOSTAK-CHRZANOWSKI A., CHRZANOWSKI A., POPOLEK E. 1995. *Modeling of Gravity Changes in Mining Areas*. Proceedings 3-rd Canadian Conf. on Computer Applications in Mineral Industry - CAMI'95, McGill University, Montreal, Oct., 22-25.
- SZOSTAK-CHRZANOWSKI A., CHRZANOWSKI A., SHENLONG K., LAMBERT A. 1996. *Finite Element Modeling of Tectonic Movements in Western Canada*. Proceedings, 6-th International FIG Symposium on Deformation Measurements, (ed. H. Pelzer and R. Heer), Hannover, 24-28 February 1992, pp. 733-744.
- SZOSTAK-CHRZANOWSKI A., MASSIÉRA M., CHRZANOWSKI A., WHITAKER C., DUFFY M. 2000. *Verification of Design Parameters of Large Earthen Dams using Deformation Monitoring Data-Potentials and Limitations*. Proceedings Canadian Dam Association, Third Annual Conference, Regina, 16-21 September, pp. 193-202.
- SZOSTAK-CHRZANOWSKI A., ORTIZ E., CHRZANOWSKI A. 2006. *Integration of In-situ Data with Modelling of Ground Subsidence in Oil Fields*. Proceedings, Geokinematischer Tag, Freiberg, Germany, 9 -10 May (in print).
- SZOSTAK-CHRZANOWSKI A., CHRZANOWSKI A., ORTIZ E. 2006. *Modeling of ground subsidence in oil fields*. Wyd. UWM Olsztyn, Tech. Sc., 9: 133-146.
- TOUILIB B.N., BONNELLI S., ANTHONIAC P., CARRERE A., DEBORDES D., LA BARBERA G., BANI A., MAZZA G. 2000. *Settlement by Wetting of the Upstream Rockfills of Large Dams*. Proceedings 53-rd Canadian Geotechnical Conference, 1: 263-270.
- VAN DER KNAAP AND VAN DER VLIS. 1967. *On the Cause of Subsidence in Oil producing Areas*. Proceedings 7-th World Pet. Congr. , Mexico City, pp. 85-95.
- VERMA N.S., PARÉ J.-J., BONCOMPAIN B., GARNEAU R., RATTUE A. 1985. *Behaviour of the LG-4 main dam*. Proceedings 11th ICSMFE, San Francisco, August 12-16. A.A. Balkema, Rotterdam, 4: 2049-2054.
- WHITAKER C, DUFFY M.A., CHRZANOWSKI A. 1999. *Installation of a Continuous Monitoring Scheme for the Eastside Reservoir Project in California*. Proceedings 9th International FIG Symposium on Deformation Measurements, Olsztyn, Poland, pp 85-97.

Translated by Authors

Accepted for print 2006.12.28

Reviewers

Janusz Badur, Henryk Budzeń, Sfefan Cacoń, Wiktor Gambin, Jerzy Jaźwiński,
Józef Kowalcuk, Marek Matczyński, Janusz Podleśny, Leszek Powierża,
Andrzej Radowicz, Dorota Witrowa-Rejchert, Ewa Wachowicz, Józef Żurek